JOURNAL OF THERMOPHYSICS AND HEAT TRANSFER
Vol. 12, No. 1, January–March 1998

Vibrational Energy Transfer Rates Using a Forced Harmonic Oscillator Model

Igor V. Adamovich*
Ohio State University, Columbus, Ohio 43210-1107
Sergey O. Macheret†
Princeton University, Princeton, New Jersey 08544
J. William Rich‡
Ohio State University, Columbus, Ohio 43210-1107
and
Charles E. Treanor§
Calspan—University at Buffalo Research Center, Buffalo, New York 14225

This paper addresses the analysis, validation, and application of analytic, nonperturbative, semiclassical vibration–translation (V–T) and vibration–vibration–translation (V–V–T) rate models for atom–diatom and diatom–diatom vibrational molecular energy transfer collisions. These forced harmonic oscillator (FHO) rate models are corrected and validated by comparison with recent experiments, and with three-dimensional semiclassical trajectory calculations for N_2–N_2, O_2–O_2, and N_2–O_2, which are considered to be the most reliable theoretical data available. A remarkably good overall agreement is shown for both the temperature and quantum number dependence of single-quantum and double-quantum V–V–T transitions in the temperature range $200 \le T \le 8000$ K and for vibrational quantum numbers $0 \le v \le 40$. It is demonstrated that the multiquantum vibrational energy transfer processes occur via a sequential FHO mechanism, as a series of virtual single-quantum steps during one collision. An important exception, asymmetric multiquantum V–V exchange at low temperatures, that occurs via a direct first-order mechanism, is discussed. Analytic thermally averaged FHO V–T and V–V rates are suggested. The FHO model gives new insight into vibrational kinetics and may be easily incorporated into kinetic modeling calculations under conditions when first-order theories are not applicable.

I. Introduction

VIBRATIONAL energy transfer in collisions of diatomic molecules plays a fundamental role in molecular lasers, gas discharges, plasma chemical reactors, high-enthalpy gas-dynamic flows, and in upper atmosphere chemistry. In these environments, it creates and maintains strongly nonequilibrium molecular vibrational energy distributions (VDFs) that induce nonequilibrium chemical reactions, electronic excitation, dissociation, and the ionization of diatomics.[1–4] The rates of these high energy threshold processes are determined by the populations of the high vibrational levels of molecules. These populations are often controlled by vibration–translation (V–T) processes

$$AB(i) + M \leftrightarrows AB(f) + M \tag{1}$$

and vibration–vibration–translation (V–V–T) processes

$$AB(i_1) + CD(i_2) \leftrightarrows AB(f_1) + CD(f_2) \tag{2}$$

involving highly vibrationally excited molecules. In Eqs. (1) and (2), AB, CD, and M represent diatomic molecules and an atom, respectively, and i_1, i_2, f_1, and f_2 are vibrational quantum numbers.

There exists an extensive literature on the experimental and theoretical study of V–T and V–V–T energy transfer.[5–10] However, experimental data for the processes [Eqs. (1) and (2)] at high quantum numbers are available only for a few species such as CO, NO, and O_2,[11–15] and only for low temperatures, up to several hundred degrees celsius. Among numerous theoretical models available in the literature, one may separate the following major approaches: 1) exact quantum calculations, 2) classical and semiclassical trajectory calculations, 3) first-order perturbation theory (FOPT), and 4) analytic nonperturbative methods.

The exact fully quantal calculations[7] are extremely computationally laborious. Therefore, they are usually made for a simplified model of collinear collision of harmonic oscillators, for low vibrational quantum numbers,[16–18] and for use as tests for more approximate approaches.

Among classical and semiclassical methods[8] we mention the semiclassical close-coupled method developed by Billing[9] for three-dimensional molecular collisions with a realistic intermolecular potential. Close-coupled trajectory calculations by this method have been performed for a number of diatomic species, including H_2, N_2, O_2, and CO, in a wide range of temperatures and vibrational quantum numbers.[19–24] Unfortunately, the direct use of this and other semiclassical methods in modeling calculations is difficult because of the considerable amount of computer time that would be required, while suggested analytic parametrization has very little or no theoretical basis.

As is well known, the FOPT, based on a collinear collision model [Schwartz-Slawsky-Herzfeld (SSH) theory, Rapp-

Presented as Paper 95-2060 at the AIAA 30th Thermophysics Conference, San Diego, CA, June 19–22, 1995; received April 3, 1997; revision received July 30, 1997; accepted for publication Aug. 5, 1997.

*Research Scientist, Department of Mechanical Engineering, 206 West 18th Avenue. Senior Member AIAA.
†Research Staff Member, Department of Mechanical and Aerospace Engineering, D410, Engineering Quadrangle. Senior Member AIAA.
‡Ralph W. Kurtz Professor, Department of Mechanical Engineering, 206 West 18th Avenue. Associate Fellow AIAA.
§Executive Staff. Fellow AIAA.

–Englander-Golden model, Sharma–Brau theory, etc.[25–30]], more or less reliably gives only the single-quantum transition probabilities [$|i-f| = 1$ in Eq. (1) or $|i_1 - f_1|, |i_2 - f_2|, |i_1 + i_2 - f_1 - f_2| \leq 1$ in Eq. (2)], for conditions such that they are much smaller than unity. The FOPT fails at high temperatures, high vibrational quantum numbers, and for multiquantum transitions, when the two-state approximation breaks down. However, the FOPT, with several a posteriori corrections, is widely used in kinetic modeling calculations, mostly because of its simplicity.

Finally, there exists a semiclassical nonperturbative analytic solution for the V–T and V–V–T transition probabilities of Eqs. (1) and (2) for a harmonic oscillator acted upon by an external exponential force.[31–33] This is the solution that is called the forced harmonic oscillator (FHO) model throughout this paper. The FHO model was originally developed for the simplified collision model, and it neglects the role of vibration–rotation coupling. However, it does take into account the coupling of many vibrational states during a collision, which is crucial not only for multiquantum processes but also for single-quantum processes at high collision velocities and high quantum numbers.[9]

The present paper addresses modifications and extensions of the FHO theory, and its validation by comparison with recent experiments and more advanced theoretical models. The main objective is development of nonperturbative analytic theory of V–V–T rates with predictive capability beyond the range of currently available experiments, which allows easy use in plasma kinetic modeling and in the modeling of gasdynamic flows.

II. FHO Transition Probabilities

The FHO theory assumes that each V–T or V–V–T transition [see Eqs. (1) and (2)] occurs as a series of virtual one-quantum steps during a single collision. The total transition probability is evaluated by adding the probability amplitudes of all energy allowed pathways. The number of pathways, not necessarily unique even for single-quantum transitions, dramatically increases with the number of accessible quantum states of a colliding system, e.g., for multiquantum transitions, diatom–diatom collisions, and also for high-energy collisions.

Summarizing the results of Kerner,[31] Treanor,[32] and Zelechow et al.,[33] one obtains the following analytical expressions for the V–T transition probabilities [see Eq. (1)] in collinear atom–diatom collisions

$$P_{VT}(i \to f, \varepsilon) = i!f!\varepsilon^{i+f}\exp(-\varepsilon)\left|\sum_{r=0}^{n}\frac{(-1)^r}{r!(i-r)!(f-r)!}\frac{1}{\varepsilon^r}\right|^2 \tag{3}$$

and for V–V–T probabilities [see Eq. (2)] in collinear diatom–diatom collisions

$$P_{VVT}(i_1, i_2 \to f_1, f_2, \varepsilon, \rho) = \left|\sum_{r=0}^{n} \mathbb{C}^{(i_1+i_2)}_{r+1,i_2+1}\,\mathbb{C}^{(f_1+f_2)}_{r+1,f_2+1} \times \exp[-i(f_1+f_2-r)\rho]\cdot P^{1/2}_{VT}(i_1+i_2-r \to f_1 + f_2 - r, 2\varepsilon)\right|^2 \tag{4}$$

In Eq. (3), i and f are the initial and final vibrational quantum states of the molecules, respectively, $n = \min(i, f)$, and ε is the average number of quanta transmitted to the initially nonvibrating oscillator. In Eq. (4), where the square root is always taken with a positive sign, i_1, i_2, f_1, and f_2 are initial and final vibrational states of colliding partners, respectively, $n = \min(i_1 + i_2, f_1 + f_2)$, ε has the same meaning as in Eq. (3), and $\mathbb{C}^{(k)}_{ij}$ is the transformation matrix. An explicit expression for the calculation of matrix $\mathbb{C}^{(k)}_{ij}$ can be found in Ref. 33.

The parameters ε and ρ in Eqs. (3) and (4) are simply related to the two-state FOPT transition probabilities $P_{FOPT}(1 \to 0)$ and $P_{FOPT}(1, 0 \to 0, 1)$. For example, for a purely repulsive exponential intermolecular potential $V(r) \sim \exp(-\alpha r)$, one has[26,27–29]

$$\varepsilon = P_{FOPT}(1 \to 0) = S_{VT}\cdot\frac{2\pi^2\omega(\tilde{m}^2/\mu)\gamma^2}{\alpha^2 h}\sinh^{-2}\left(\frac{\pi\omega}{\alpha\bar{v}}\right) \tag{5}$$

$$\rho = (4\cdot P_{FOPT}(1, 0 \to 0, 1))^{1/2} = \left(S_{VV}\cdot\frac{4\tilde{m}^2\gamma_1^2\gamma_2^2}{\mu_1\mu_2}\frac{\alpha^2\bar{v}^2}{\omega_1\omega_2}\right)^{1/2} \cong \left(S_{VV}\cdot\frac{\alpha^2\bar{v}^2}{\omega_1\omega_2}\right)^{1/2} \tag{6}$$

In Eqs. (5) and (6), ω, ω_1, and ω_2 are oscillator frequencies; $\tilde{m}$ is the collision-reduced mass; μ, μ_1, and μ_2 are oscillator reduced masses, $\gamma = \gamma_1 = m_B/(m_A + m_B)$; $\gamma_2 = m_C/(m_C + m_D)$; and $\bar{v}$ is the symmetrized collision velocity. In the present paper, we define $\bar{v}$ as an arithmetic average of the initial and the final collision velocities. As in any other semiclassical rate model, symmetrization is used to enforce energy conservation and detailed balance. S_{VT} and S_{VV} are corrective steric factors, $0 < S < 1$, originating from the noncollinear nature of collisions, and will be discussed later. To take into account the effect of the intermolecular attraction on the V–T relaxation at low temperatures, when this effect might be substantial, instead of Eq. (5) one should use the expression

$$\varepsilon = P_{FOPT}(1 \to 0) = S_{VT}\cdot\frac{8\pi^2\omega(\tilde{m}^2/\mu)\gamma^2}{\alpha^2 h}\frac{\cosh^2\left[\frac{(1+\phi)\pi\omega}{\alpha\bar{v}}\right]}{\sinh^2\left(\frac{2\pi\omega}{\alpha\bar{v}}\right)} \tag{7}$$

obtained in Ref. 34 for the intermolecular Morse potential. In Eq. (7)

$$\phi = (2/\pi)\tan^{-1}[(2E/\tilde{m}\bar{v}^2)^{1/2}] \tag{8}$$

where E is the Morse potential well depth.

The V–T and V–V–T probabilities [Eqs. (3–6)], have been compared with exact quantum calculations for collinear geometry and show very good agreement at low quantum states and high collision energies, including multiquantum transitions.[35–39]

To use the FHO transition probabilities for simulation of vibrational relaxation of real gases (including transitions among high vibrational quantum numbers), some obvious corrections have to be made. First, we suggest determining the steric factors S_{VT} and S_{VV} from the comparison of the first-order probabilities $P_{FOPT}(1 \to 0)$ and $P_{FOPT}(1, 0 \to 0, 1)$ of Eqs. (5) and (6) to the results of more advanced three-dimensional close-coupled calculations at low collision velocities. We realize that these parameters do not reflect the dynamics of a real collision and are purely phenomenological. The only justification for their use is that, as we will show here, they work quite satisfactorily, being the same for several molecular systems in a wide temperature range.

Second, to generalize Eq. (4) for the case of nonresonance V–V transitions and for V–V exchange between different species, we use the two-state FOPT result,[6] replacing ρ given by Eq. (6) with the expression

$$\rho_\xi = \rho\cdot\frac{\xi}{\sinh(\xi)}, \qquad \xi = \frac{2|\omega_1 - \omega_2|}{\alpha\bar{v}} = \frac{2\Omega}{\alpha\bar{v}} \tag{9}$$

In the present paper, we use the correction of Eq. (9) rather than the results of Ref. 39 for asymmetric diatom–diatom col-

lisions between different species, because the results of Ref. 39 have not been presented in a closed analytical form.

Finally, to account for the anharmonicity of a real oscillator, as a first approximation we use a frequency corrected harmonic oscillator, replacing the frequencies ω, ω_1, ω_2 in Eqs. (5–7) and (9) by average frequencies

$$\omega = \begin{vmatrix} |(E_i - E_f)/(i - f)|, & i \neq f \\ |E_{i+1} - E_i|, & i = f \end{vmatrix} \qquad E_i = \omega_e i \cdot [1 - x_e(i + 1)]$$
$$\Omega = |\omega_1 - \omega_2| \tag{10}$$

where ω_e and x_e are vibrational quantum and anharmonicity of a molecule, respectively. Assumption (10) has been made also by Billing and Fisher[19,20] in their close-coupled calculations of V–T and V–V rates. They found that it weakly affects the values of the coupling matrix elements, compared to those of the exact Morse oscillator, and results in less than a 30% correction to the rates.

III. Thermally Averaged FHO Rates

For modeling calculation purposes, the thermally averaged FHO probabilities can be obtained using asymptotic representation of the probabilities given by Eqs. (3) and (4). It was first shown in Ref. 6 that the rather cumbersome analytical forms of Eqs. (3) and (4) can be simplified by the following analytic formulas. For the V–T probabilities of Eq. (3) and for pure V–T probabilities ($M = i_2 = f_2$) of Eq. (4) we can use

$$P_{VT}(i \to f, \varepsilon) = P_{VT}(i, M \to f, M, \varepsilon) \cdot \exp(\varepsilon) = J_s^2[2(n_s \varepsilon)^{1/2}] \tag{11}$$

where

$$s = |i - f|, \qquad n_s = \left[\frac{\max(i, f)!}{\min(i, f)!}\right]^{1/s} \tag{12}$$

and for the pure V–V probabilities ($i_1 + i_2 = f_1 + f_2$) of Eq. (4), we can use

$$P_{VV}(i_1, i_2 \to f_1, f_2, \rho) = J_s^2\{2[n_s^{(1)} \cdot n_s^{(2)} \cdot \rho_\xi^2/4]^{1/2}\} \tag{13}$$

where

$$s = |i_k - f_k|, \qquad n_s^{(k)} = \left[\frac{\max(i_k, f_k)!}{\min(i_k, f_k)!}\right]^{1/s}, \qquad k = 1, 2 \tag{14}$$

In Eqs. (11) and (13), J_s is the Bessel function of the sth order. Using the Bessel function expansion in a series[40]

$$J_s(z) = \left(\frac{z}{2}\right)^s \sum_{k=0}^{\infty} \frac{(-1)^k}{k!\Gamma(s + k + 1)} \left(\frac{z}{2}\right)^{2k} \cong \left(\frac{z}{2}\right)^s \frac{1}{s!} \exp\left(-\frac{z^2}{4(s + 1)}\right) \tag{15}$$

and using the simplifications of Eqs. (11) and (13), one obtains the following approximation of probabilities (3) and (4)

$$P_{VT}(i \to f) = P_{VT}(i, M \to f, M, \varepsilon) \cdot \exp(\varepsilon) = \frac{(n_s)^s}{(s!)^2} \cdot \varepsilon^s \cdot \exp\left(-\frac{2n_s}{s + 1} \varepsilon\right) \tag{16}$$

$$P_{VV}(i_1, i_2 \to f_1, f_2) \cong \frac{[n_s^{(1)} n_s^{(2)}]^s}{(s!)^2} \cdot \left(\frac{\rho_\xi^2}{4}\right)^s \cdot \exp\left[-\frac{2n_s^{(1)} n_s^{(2)}}{s + 1} \frac{\rho_\xi^2}{4}\right] \tag{17}$$

The approximation of Eq. (16) applied to atom–diatom collisions works extremely well. On the other hand, expressions (16) and (17) for diatom–diatom collision are valid only as long as the V–V–T probabilities are separable into two independent V–T (ε-dependent) and V–V (ρ-dependent) modes. One can see from Eqs. (3) and (4) that this is not so at very high collision velocities, when the parameters ε and ρ may both become comparable to unity [see Eqs. (5) and (6)]. From Eqs. (3) and (4), one can show that for diatom–diatom collisions, Eq. (16) is valid if

$$\rho^2/4 << 1 \tag{18}$$

while Eq. (17) is correct if

$$\varepsilon << \rho/2s \tag{19}$$

If conditions (18) and (19) do not hold, then the probabilities depend on both parameters ε and ρ (V–T and V–V modes become mixed), and the general equation, (4), should be used.

Following the usual Landau–Teller–Herzfeld procedure,[5] one can average the probabilities [Eqs. (16) and (17)] over the one-dimensional Boltzmann distribution

$$k(T) = Z\left(\frac{\tilde{m}}{kT}\right) \int_0^\infty P(\bar{v}) \cdot \exp\left(\frac{-\tilde{m}v^2}{2kT}\right) v \, dv \tag{20}$$

to obtain thermally averaged V–T and V–V rates. In Eq. (20), Z is the gas-kinetic collision frequency. For V–T processes, the integral in Eq. (20) is evaluated by the steepest descent method, assuming $\pi\omega >> \alpha\bar{v}$ in Eq. (5) ($\pi\omega >> \alpha\bar{v}$ for all except the most energetic collisions, which only play a significant role at thermal energies $T \geq 10^5$ K). The result of this steepest descent integration is

$$k(i \to f, T) = Z \cdot \left(\frac{2\pi}{3 + \delta}\right)^{1/2} \frac{\left(n_s S_{VT} \dfrac{\theta'}{\theta}\right)^s}{(s!)^2} C_{VT} \left(\frac{s^2\theta'}{T}\right)^{1/6} \times \exp\left[-\left(\frac{s^2\theta'}{T}\right)^{1/3} (1 - \phi_m)^{2/3} \times \left(\frac{C_{VT}^2}{2} + \frac{1}{C_{VT}}\right) - s(1 - C_{VT}^3)\right] \exp\left(\frac{\theta s}{2T}\right) \tag{21}$$

where

$$\theta' = \frac{8\pi^2\omega^2(\tilde{m}^2/\mu)\gamma^2}{\alpha^2 k}, \qquad \theta = \frac{h\omega}{k} \tag{22}$$

$$\delta = \frac{1 - C_{VT}^3}{C_{VT}^3} \frac{2\pi\omega}{\alpha v_{m0} C_{VT}}, \qquad \phi_m = \frac{2}{\pi} \tan^{-1}[(2E/\tilde{m}v_{m0}^2)^{1/2}] \tag{23}$$

and C_{VT} determines the collision velocity v_m at which the integrand in Eq. (20) reaches the maximum

$$C_{VT} = \frac{v_m}{v_{m0}} \cong \left[1 - \frac{1}{s}\left(\nu + \frac{2n_s}{(s + 1)}\right) S_{VT} \frac{\theta'}{\theta} \exp\left(-\frac{2\pi\omega}{\alpha v_{m0} C_{VT}}\right)\right]^{1/3} \tag{24}$$

where $\nu = 0$ for atom–diatom collisions and $\nu = 1$ for diatom–diatom collisions. In Eqs. (23) and (24), v_{m0} is the Landau–Teller most effective velocity

$$v_{m0} = \left(\frac{2\pi\omega s k T}{\alpha\tilde{m}}\right)^{1/3} \tag{25}$$

Note that factor ϕ_m in Eq. (21) determines the effect of the

intermolecular attraction on the V–T relaxation rate [cf. Eq. (7)], which makes Eq. (21) applicable also at low temperatures.

Similarly, for far-from-resonance V–V processes ($\pi\Omega >> \alpha\bar{v}$), one obtains from Eqs. (6) and (17)

$$k(i_1, i_2 \to f_1, f_2, T) = Z\cdot\left(\frac{2\pi}{3+\delta}\right)^{1/2}\frac{[n_s^{(1)}n_s^{(2)}]^s}{(s!)^2}\left(\frac{S_{VV}\pi^2\Omega^2}{\omega^2}\right)^s C_{VV}\left(\frac{s^2\theta'}{T}\right)^{1/6} \times \exp\left[-\left(\frac{s^2\theta'}{T}\right)^{1/3}\left(\frac{C_{VV}^2}{2}+\frac{1}{C_{VV}}\right)-s(1-C_{VV}^3)\right] \times\exp\left(\frac{\Omega s}{2kT}\right) \tag{26}$$

where now

$$\theta' = \frac{4\pi^2\Omega^2\tilde{m}}{\alpha^2 k}, \qquad \delta = \frac{1-C_{VV}^3}{C_{VV}^3}\frac{2\pi\Omega}{\alpha v_{m0}C_{VV}} \tag{27}$$

$$C_{VV} = \frac{v_m}{v_{m0}} = \left[1-\frac{2n_s^{(1)}n_s^{(2)}}{s(s+1)}S_{VV}\frac{\pi^2\Omega^2}{\omega^2}\exp\left(-\frac{2\pi\Omega}{\alpha v_{m0}C_{VV}}\right)\right]^{1/3} \tag{28}$$

$$v_{m0} = \left(\frac{2\pi\Omega skT}{\alpha\tilde{m}}\right)^{1/3} \tag{29}$$

Transcendental Eqs. (24) and (28) each have a single root and in practical calculations can be easily solved by the Newton method. At $s = 1$ and $\varepsilon << 1$, $\rho << 1$, $C_{VT} \cong C_{VV} \cong 1$, and Eqs. (21) and (26) reduce to give the result of the SSH theory.[5]

Finally, for resonance V–V energy exchange ($\Omega = 0$), exact integration of Eq. (20), where $P(\bar{v})$ is given by Eqs. (6) and (17), gives

$$k(i_1, i_2 \to i_2, i_1, T) = Z\cdot\frac{n_s^{2s}}{s!}\frac{\langle P_{1\to 0}^{0\to 1}\rangle^s}{\left(1+\frac{2n_s^2\cdot\langle P_{1\to 0}^{0\to 1}\rangle}{s+1}\right)^{s+1}} \tag{30}$$

where

$$\langle P_{1\to 0}^{0\to 1}\rangle = \frac{S_{VV}\alpha^2 kT}{2\omega^2\tilde{m}} \tag{31}$$

is the thermally averaged FOPT probability of Eq. (6).[27–29] Again, Eq. (30) gives the result of the SSH theory if $s = 1$, $\langle P_{1\to 0}^{0\to 1}\rangle << 1$. The gap between the far-from-resonance [Eq. (26)] and the exact resonance [Eq. (30)] V–V rates can be filled by multiplying the resonance rate [Eq. (30)] by the energy defect function $G(\lambda)$, similar to that suggested by Keck and Carrier[41]

$$G(\lambda) = \tfrac{1}{2}(3 - e^{-(2/3)\lambda})e^{-(2/3)\lambda} \tag{32}$$

where λ is proportional to the vibrational energy defect ΔE,

$$\lambda = \frac{1}{\pi\sqrt{2}}\left(\frac{\theta'}{T}\right)^{1/2}\frac{|\Delta E|}{s\cdot k\theta} = \frac{1}{\pi\sqrt{2}}\left(\frac{\theta'}{T}\right)^{1/2}\frac{\Omega}{\omega} \tag{33}$$

and that provides very good accuracy both for single-quantum and multiquantum transitions, compared to the rates, obtained by numerical integration of the probabilities [Eq. (4)] over the Boltzmann distribution [Eq. (20)].

From Eqs. (18) and (25) one can easily estimate that Eq. (21) for diatom–diatom collisions can be used if

$$T << T_{VT} \sim \theta'/s \tag{34}$$

where $\theta' \sim 10^7$ K for N_2 and O_2. A similar estimate, using Eq. (19) and the most probable velocity for resonance V–V processes

$$v_m \sim [(2s+1)\cdot kT/\tilde{m}]^{1/2} \tag{35}$$

shows that the V–V rates of Eq. (30) can be used if

$$s\frac{\theta'}{\theta}x\cdot e^{-x} << 1, \qquad T = \frac{\theta'}{(2s+1)x^2} \tag{36}$$

This estimate gives $T << T_{VV} \sim 10^5/(2s+1)$ K for nitrogen. At higher temperatures, the V–V mode becomes strongly affected by the V–T mode, and rates of Eqs. (26), (30), and (32) should not be used. Calculations using Eqs. (3) and (4) show that at $T >> T_{VV}$, the V–V–T processes occur as two independent V–T processes, so that the probabilities can be factorized

$$P(i_1, i_2 \to f_1, f_2) \cong P(i_1, f_1)\cdot P(i_2, f_2) \tag{37}$$

Note that, according to our assumption (10), parameters ω and Ω, used throughout this section, are given by Eq. (10).

Finally, comparison of the FHO and the FOPT probabilities for the multiquantum transitions (see Appendix) proves that both V–T and V–V multiquantum processes principally occur via a sequential FHO mechanism, rather than via a straightforward FOPT mechanism. As a result, we obtain simple analytic formulas for nonperturbative V–T and V–V rate constants that are applicable up to very high temperatures, at high vibrational quantum numbers, and also for multiquantum vibrational energy transfer.

IV. Validation and Discussion

Before we discuss the validation of the FHO model, described in Sec. III, it is necessary to outline the area of its applicability. First of all, because it remains based on the simple collision model, the FHO model does not account for strong vibration–rotation coupling, important for vibrational energy transfer in hydrogen and in hydrogen halides.[42] Further, the model cannot be expected to predict V–V–T probabilities for reactive collisions or for collisions involving nonadiabatic electronic transitions, as presumably occurs in NO–NO.[43] Also, the FHO model, in its present form, cannot predict the probabilities of transitions induced by multipole–multipole attractive forces, which are known to strongly affect the V–V probabilities for CO–CO and CO–N_2 at low temperatures.[23,24] However, it has been previously shown[44] that the FHO V–T and V–V–T scaling relationships given by Eqs. (3) and (4) are independent of the intermolecular potential. The interaction potential determines only the parameters ε and ρ in Eqs. (3) and (4). The scaling relations (3) and (4) have also been shown to agree well with the exact quantum calculations[45–47] for the Lennard–Jones 12-6 potential, which accounts for the long-range attraction.[38] In this case, the parameters ε and ρ in Eqs. (3) and (4) are also calculated for the same 12-6 potential, rather than taken from Eqs. (5–7). Therefore the FHO model, with properly evaluated ε and ρ, might be generalized for heteronuclear diatomics. Finally, the FHO model is expected to work reasonably well for relatively heavy homonuclear diatomics, such as N_2 and O_2.

To validate the use of the corrected FHO model for kinetic modeling calculations, it has to be compared with experimental data, or, if they are not available, with more advanced theoretical models. Experimental information for the high vibrational level transition probabilities in homonuclear diatomics is limited to recent stimulated emission pumping (SEP) results for O_2–O_2 and N_2–O_2.[13–15] Three-dimensional quantum calculations for these molecules, to our knowledge, are not available. However, there exists an extensive database on V–T and

V–V rates for diatomic molecules, obtained by Billing,[9] using close-coupled, semiclassical, three-dimensional trajectory calculations. This is considered to be the most comprehensive and reliable database available at this time. For validation of the FHO model, in addition to the experimental data,[13–15] we used the results of these calculations for three molecular systems, N_2–N_2,[20] O_2–O_2,[21] and N_2–O_2.[22]

In our calculations, we use an intermolecular Morse potential with the exponential repulsion parameter $\alpha = 4.0\ A^{-1}$ and a well depth $E = 200$ K, chosen to fit the potentials used in Refs. 20–22. Parameters ε and ρ in Eqs. (3) and (4) have been calculated using Eqs. (6), (7), and (9). The corrective steric factors S, used in Eqs. (5–7) (Sec. II), have been obtained from matching the two FHO probabilities at relatively low collision velocities, when the V–T and V–V modes are separable

$$P(1, 0 \rightarrow 0, 0) \cong S_{VT} \cdot \varepsilon$$
$$P(1, 0 \rightarrow 0, 1) \cong S_{VV} \cdot \rho^2/4 \quad \text{at low } v \tag{38}$$

to the results of Refs. 20 and 21. It has been found that the values $S_{VT} \cong 0.5$ and $S_{VV} \cong 0.04$ provide very good agreement between the FHO model probabilities and the three-dimensional calculations for N_2–N_2 and O_2–O_2 in a wide temperature range. In other words, the steric factors have been found to be temperature independent and approximately the same for both molecules. These values of S_{VT} and S_{VV} are used in all subsequent calculations, and they are the only fitting parameters in the present model.

The following series of figures compares the results of the FHO model, calculated using Eqs. (21) and (30–33), to those of Billing and co-workers (Refs. 20–22) and to the experimental data.

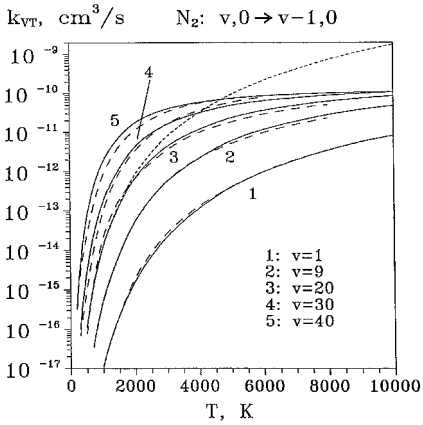

Fig. 1 Single-quantum V–T rates for N_2–N_2. ——, FHO model; – – –, calculations of Ref. 20; · · · · ·, FOPT, $k_{VT}(20 \rightarrow 19)$.

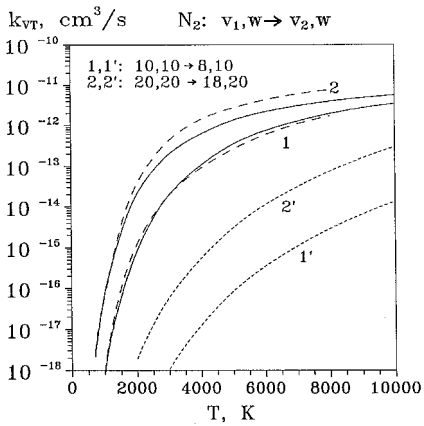

Fig. 2 Double-quantum V–T rates for N_2–N_2. ——, FHO model; – – –, calculations of Ref. 20; · · · · ·, FOPT, $k_{VT}(10 \rightarrow 8)$ and $k_{VT}(20 \rightarrow 18)$.

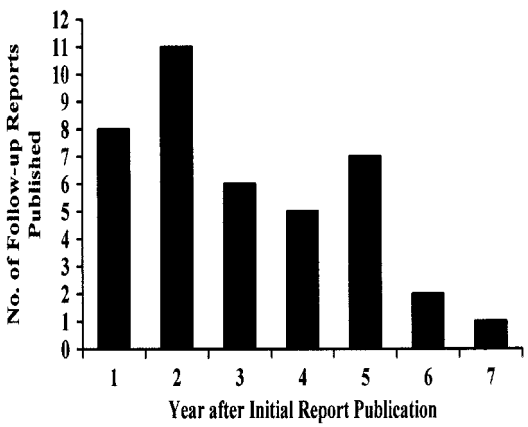

Fig. 3 Single-quantum nonresonance V–V rates for N_2–N_2. ——, FHO model; – – –, calculations for Ref. 20. 1, T = 200 K; 2, T = 300 K; 3, T = 500 K; 4, T = 1000 K; 5, T = 2000 K; 6, T = 10,000 K.

A. N_2–N_2

Figure 1 shows the single-quantum V–T rates for N_2–N_2 and those reported by Billing and Fisher.[20] The agreement is remarkably good in the entire temperature range 200–8000 K, for vibrational levels $v \leq 40$. This behavior is quite different from that of the two-state SSH theory, which does not consider multiquantum relaxation properly and therefore overpredicts the single-quantum V–T rates at high temperatures and at high vibrational levels (see Fig. 1). The FHO double-quantum V–T rates for high quantum numbers also agree well with Billing's results (Fig. 2), whereas the corresponding FOPT rates are smaller by several orders of magnitude. This fact illustrates the dominance of the sequential FHO mechanism of multiquantum V–T relaxation over the straightforward FOPT mechanism, as discussed in Sec. III.

Figures 3–5 show the single-quantum and double-quantum V–V rates. The overall agreement between the FHO model and the Billing data for the V–V mode, although still satisfactory, is not as good as for the V–T mode. This may be explained by a stronger effect of vibration–rotation coupling on the V–V rates. From Fig. 5, it is clear that the double-quantum V–V processes also preferentially occur by the sequential mechanism, as predicted in Sec. III, because the FOPT rates are again much smaller than the FHO rates, especially at high temperatures.

Note that the V–V probabilities[33] that can be obtained from Eq. (4) by taking all $P_{VT} = 1$ have been previously compared

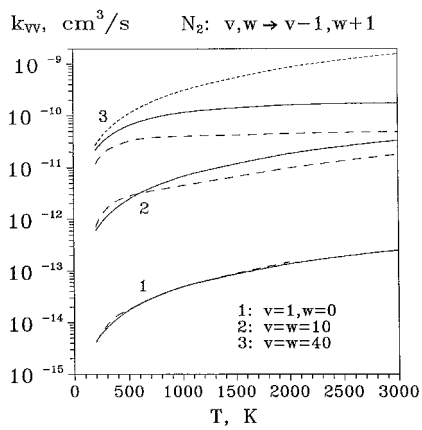

Fig. 4 Single-quantum near-resonance V–V rates for N_2–N_2. ——, FHO model; – – –, calculations of Ref. 20; · · · · ·, FOPT, $k_{VV}(40, 40 \rightarrow 39, 41)$.

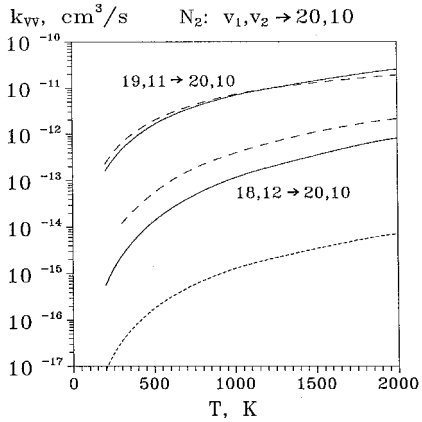

Fig. 5 Single- and double-quantum nonresonance V–V rates for N_2–N_2. ——, FHO model; – – –, calculations of Ref. 20; · · · · ·, FOPT, $k_{VV}(18, 12 \rightarrow 20, 10)$.

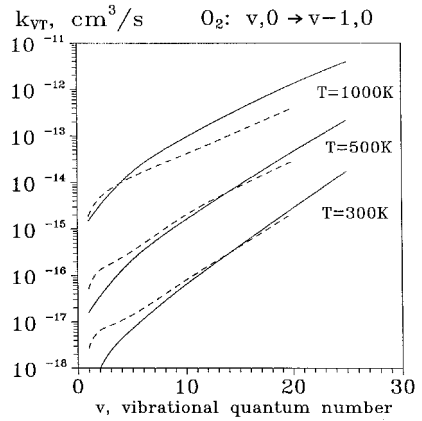

Fig. 6 Single-quantum V–T rates for O_2–O_2. ——, FHO model; – – –, calculations of Ref. 21.

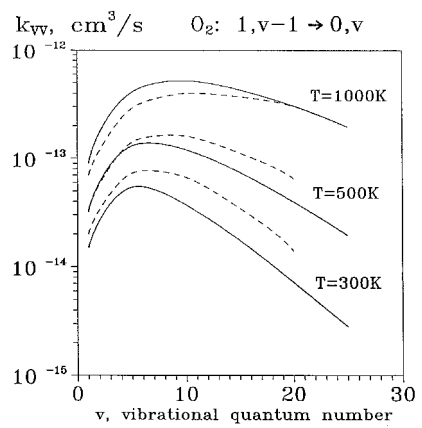

Fig. 7 Single-quantum nonresonance V–V rates for O_2–O_2. ——, FHO model; – – –, calculations of Ref. 21.

with close-coupled calculations[20] for the single-quantum V–V transitions in nitrogen, showing good agreement.[49] However, in Ref. 49 the probabilities are numerically averaged over the Boltzmann distribution, so that the results are not presented in a closed analytic form.

B. O_2–O_2

The comparison of the FHO and Billing's models[21,22] for O_2–O_2 and N_2–O_2, discussed further, is especially challenging. The recent calculations for these systems, performed by Billing and his co-workers[21,22] no longer use the frequency corrected harmonic oscillator assumption [see Eq. (9)] suggested in the

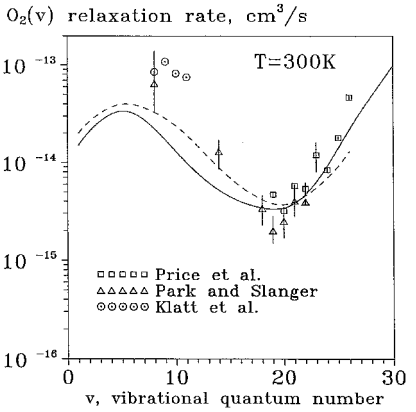

Fig. 8 Relaxation rate of the vibrationally excited oxygen. ——, FHO model; – – –, calculations of Ref. 21.

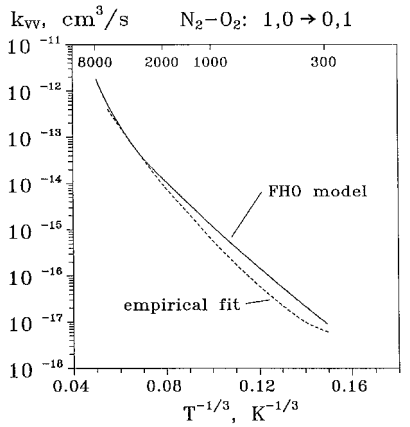

Fig. 9 V–V rate for N_2–O_2 (1, 0 → 0, 1). ——, FHO model; best fit to experimental data, Ref. 51.

earlier H_2–H_2 and N_2–N_2 studies.[19,20] Instead, more realistic Morse oscillator matrix elements are used. Note that the inclusion of anharmonicity in collinear semiclassical calculations results in a substantial decrease of the V–T probabilities compared to those for harmonic oscillator, by factors of 0.1 to 0.01, because of the deviation of the diagonal matrix elements from unity.[48] However, Figs. 6 and 7, showing the satisfactory agreement between the two models, demonstrate that this effect is obviously less pronounced for three-dimensional trajectories. A similar result was previously obtained in a purely classical three-dimensional trajectory calculation for O_2–Ar.[50] Also, the two models agree well with the recent SEP measurements of the O_2 relaxation rate.[13–15] Figure 8 shows both experimental data and theoretical relaxation data, calculated by adding the rates of the V–T and the nonresonance V–V processes.

C. N_2–O_2

Figure 9 compares the rate of the V–V exchange process

$$N_2(1) + O_2(0) \rightarrow N_2(0) + O_2(1) \qquad (39)$$

calculated by the FHO model, and best fit to the experimental data,[51] in a temperature range $300 \leq T \leq 6000$ K. Also, Figs. 10–12 show the results of comparison of the FHO single-quantum V–T and V–V rates, as well as double-quantum V–T rates in N_2–O_2, with the recently published data by Billing.[22] As one can see, the agreement between the two models is, again, quite satisfactory. However, the present FHO model rates fail to agree with data for the asymmetric single/double-quantum V–V exchange at $T = 300$ K

$$O_2(v + 1) + N_2(0) \rightarrow O_2(v - 1) + N_2(1) \qquad (40)$$

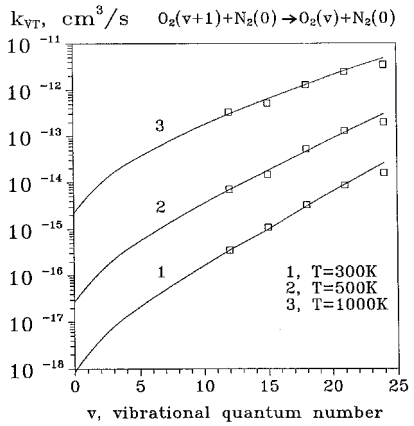

Fig. 10 Single-quantum V–T rates for N_2–O_2. ——, FHO model; □, calculations of Ref. 22.

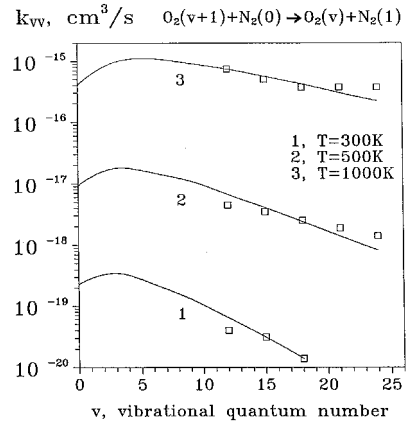

Fig. 11 Single-quantum V–V rates for N_2–O_2. ——, FHO model; □, calculations of Ref. 22.

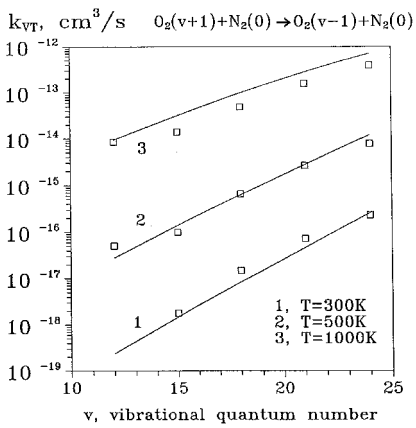

Fig. 12 Double-quantum V–T rates for N_2–O_2. ——, FHO model; □, calculations of Ref. 22.

shown in Fig. 13. Results of the present FHO model are strikingly different both from the recent SEP experiment[14] and from Billing's results,[22] being about 10 orders of magnitude smaller. Interestingly enough, the probability of process (40), calculated by the FOPT [see also Eqs. (A2), (A3), (6), and (10)]

$$P_{\text{FOPT}}(v+1,0 \rightarrow v-1,1) = v(v+1)\frac{x_e(O_2)}{4} S_{VV} \frac{\alpha^2 \bar{v}^2}{4\omega_{O_2}\omega_{N_2}} \frac{\xi^2}{\sinh^2(\xi)}, \qquad \xi = \frac{2\Omega}{\alpha \bar{v}} \tag{41}$$

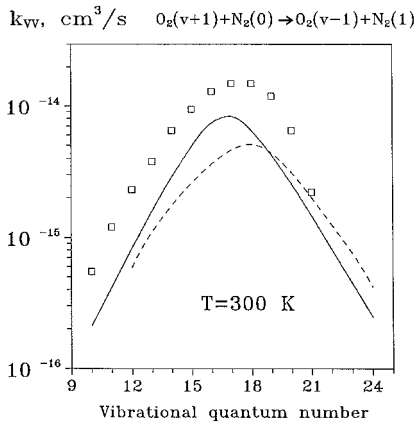

Fig. 13 Double-quantum V–V rates for N_2–O_2 at T = 300 K. ——, FOPT; - - -, calculations of Ref. 22; □, experimental data.[14] FHO rates, being about 10 orders of magnitude less than the experimental rates, are not shown.

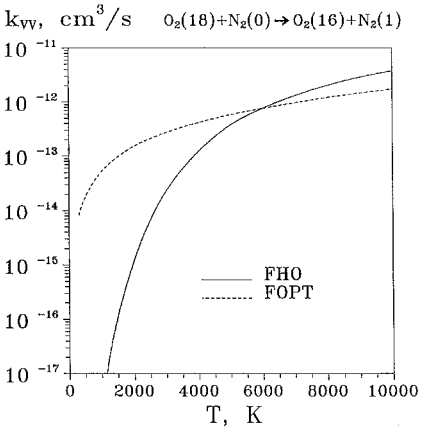

Fig. 14 Near-resonance double-quantum V–V rates for N_2–O_2 as a function of temperature. ——, FHO model; · · · · ·, FOPT.

where $\omega_{O_2} = (E_{v+1} - E_v)/h$, $\omega_{N_2} = (E_1 - E_0)/h$, and $\Omega = |\omega_{O_2} - \omega_{N_2}|$, agrees well with the experimental data and Billing's calculations[22] (see Fig. 13). The failure of the FHO theory, compared to the successful prediction of the FOPT, suggests that process (40) occurs via a straightforward pathway $(v+1, 0) \rightarrow (v-1, 1)$, rather than via the most probable FHO pathways

$$(v+1, 0) \xrightarrow{V-T} (v, 0) \xrightarrow{V-V} (v-1, 1) \tag{42}$$

or

$$(v+1, 0) \xrightarrow{V-V} (v, 1) \xrightarrow{V-T} (v-1, 1) \tag{43}$$

One can see that each of the pathways [Eqs. (42) and (43)] includes a pure V–T virtual step, which has a very low probability amplitude at room temperature and serves as a bottleneck for the entire pathway, with a total probability being approximately [see Eqs. (6), (10), (16), and (17)]

$$P_{\text{FHO}} \sim P_{\text{VT}} \cdot P_{\text{VV}} \leq v\varepsilon \cdot v(\rho/2)^2 \tag{44}$$

where ε and ρ are given by Eqs. (5) and (6). On the other hand, the FOPT probability (42) substantially increases as the vibrational energy defect in the process (40) becomes small ($\Delta E/k \cong 30$ K at $v = 17$). For the near-resonance process (40), one obtains the ratio

$$\frac{P_{\text{FOPT}}}{P_{\text{FHO}}} \geq \frac{x_e}{4\varepsilon} \tag{45}$$

which is much greater than unity at temperatures lower than $T \sim 5000$ K. At higher temperatures, when V–T probabilities sharply increase, the bottleneck no longer exists, and therefore the FHO and the FOPT rates become comparable (see Fig. 14). This example shows that for asymmetric close-to-resonance multiquantum processes at low temperatures, such as process (40), the direct FOPT mechanism dominates the sequential FHO mechanism.

Analytic expressions for the FHO V–T and V–V rates (21), (26), and (30), derived in Sec. III, can be easily used in kinetic modeling calculations and incorporated into existing computer codes. Such calculations have been recently performed for nonequilibrium chemically reacting gas flows behind shock waves.[52,53] To account for first-order multiquantum energy transfer processes, similar to the process of Eq. (40), we recommend the use of a simple superposition of the FHO and FOPT rates models. However, when using the FOPT, one has to make sure that all the FOPT probabilities are much smaller than unity, so that the theory is applicable.

V. Summary

In the present paper, we have analyzed the nonperturbative semiclassical analytic V–T and V–V–T rate models, previously suggested for the forced harmonic oscillator. The models are corrected for three-dimensional collisions, anharmonicity of the oscillator, and for collisions between oscillators with different frequencies. The FHO probabilities are averaged over the Boltzmann distribution to provide analytic V–T and V–V rates for single-quantum and multiquantum processes, including high temperatures. The corrected FHO model is validated by comparison with three-dimensional semiclassical trajectory calculations and with the recent experimental data for the three molecular systems, N_2–N_2, O_2–O_2, and N_2–O_2. Remarkably good overall agreement is shown, both for the temperature and quantum number dependence of single-quantum and double-quantum V–T and V–V transitions, in the temperature range $200 \leq T \leq 8000$ K, and for the vibrational quantum numbers $0 \leq v \leq 40$.

It is shown that the multiquantum V–T and V–V processes occur via a sequential FHO mechanism, as a series of virtual single-quantum steps during one collision, rather than via the direct FOPT mechanism. However, it is demonstrated that for the specific case of asymmetric near-resonance multiquantum V–V exchange at low temperatures, FHO theory gives much too small a result, and the rate of these processes may be successfully predicted by the FOPT. For practical calculations, the superposition of the two models is recommended.

The FHO model gives new insight into mechanisms of vibrational relaxation and, being analytic, may be used for kinetic modeling calculations at conditions where first-order theories are known to be inapplicable. Fortran subroutines used for the calculations of the rates discussed in the present paper can be easily incorporated into existing computer codes and are available upon request.

Appendix: Comparison of FOPT and FHO Probabilities

Let us use the FOPT for calculation of the multiquantum V–T and V–V probabilities, thereby formally assuming a unique straightforward two-state transition mechanism (i_1, $i_2 \rightarrow f_1$, f_2). Then, for the exponential repulsive potential $V(r) \sim \exp(-\alpha r)$, this will give the following result:

$$P_{\mathrm{FOPT}}(i \rightarrow f) = S_{\mathrm{VT}} \cdot (n_s)^s \cdot x_e^{s-1} \frac{\theta'}{4\theta} \sinh^{-2}\left(\frac{\pi\omega s}{\alpha\bar{v}}\right) \qquad \text{(A1)}$$

$$P_{\mathrm{FOPT}}(i_1, i_2 \rightarrow f_1, f_2) = [n_s^{(1)} n_s^{(2)}]^s \cdot \frac{x_e^{2s-2}}{s^4} \frac{\alpha^2 \bar{v}^2}{4\omega_1\omega_2} \qquad \text{(A2)}$$

where θ' and θ are given by Eq. (22), $\theta'/\theta \sim 10^3$, $x_e \sim 10^{-2}$ for N_2–N_2 [see Eq. (22)]. In Eqs. (A1) and (A2), we used the following approximation for the Morse oscillator linearized coupling matrix elements:

$$\langle i|\alpha\gamma x|f\rangle^2 = \frac{x_e^{s-1}}{s^2}\left(\frac{n_s}{1 - x_e n_s}\right)^s \langle 1|\alpha\gamma x|0\rangle^2 \cong (n_s)^s \frac{x_e^{s-1}}{s^2} \frac{\alpha^2 h^2 \gamma^2}{2\mu h\omega} \qquad \text{(A3)}$$

which can be easily obtained from the general expression for the repulsive potential.[48] Comparing Eqs. (16) and (A1), and using Eq. (5), at $\pi\omega >> \alpha\bar{v}$ one obtains an estimate for the ratio of the FHO and FOPT V–T probabilities

$$\frac{P_{\mathrm{VT}}^{\mathrm{FHO}}}{P_{\mathrm{VT}}^{\mathrm{FOPT}}} \cong \frac{1}{(s!)^2}\left(\frac{S_{\mathrm{VT}}\theta'}{x_e\theta}\right)^{s-1} \sim \frac{1}{(s!)^2} 10^{5(s-1)} \qquad \text{(A4)}$$

The fact that for $s > 1$ the FHO probabilities are much greater than those calculated by the FOPT shows that the sequential FHO mechanism is clearly dominant for the multiquantum V–T transitions. A similar estimate can be easily obtained for far-from-resonance V–V processes ($\pi\Omega >> \alpha\bar{v}$). Finally, for resonance V–V processes ($\Omega = 0$) one obtains an estimate for the ratio of the thermally averaged FHO and FOPT probabilities from Eqs. (6), (17), (20), and (A2)

$$\frac{\langle P_{\mathrm{VV}}^{\mathrm{FHO}}\rangle}{\langle P_{\mathrm{VV}}^{\mathrm{FOPT}}\rangle} \cong \frac{s^4}{s!}\left(\frac{S_{\mathrm{VV}}\alpha^2 kT}{2\omega^2 x_e^2 \tilde{m}}\right)^{s-1} = \frac{s^4}{s!}\left(\frac{\langle P_{1\rightarrow 0}^{0\rightarrow 1}\rangle}{x_e^2}\right)^{s-1} \qquad \text{(A5)}$$

where $\langle P_{1\rightarrow 0}^{0\rightarrow 1}\rangle$ is given by Eq. (31). At $s > 1$, this ratio is greater than unity if $\langle P_{1\rightarrow 0}^{0\rightarrow 1}\rangle \geq 10^{-4}$, which is true for molecules such as N_2 and O_2, except for at low temperatures, $T \leq 300$ K.[20,21] Therefore, at higher temperatures, V–V exchange also occurs principally by the FHO mechanism.

Acknowledgments

This work was supported by NASA SBIR Research Grant NAS1-20140 and by the Air Force Office of Scientific Research Space Propulsion and Power Program, Grant F49620-96-1-0184. We also express our gratitude to I. K. Dmitrieva, S. K. Pogrebnya, and P. I. Porshnev for drawing our attention to their paper, where they applied the results of the FHO theory to evaluate the single-quantum V–V rates.

References

[1]Gordiets, B. F., Osipov, V. A., and Shelepin, L. A., *Kinetic Processes in Gases and Molecular Lasers*, Gordon and Breach, London, 1988, Chaps. 3 and 4.

[2]Rusanov, V. D., and Fridman, A. A., *Physics of Chemically Active Plasmas*, Nauka, Moscow, 1984, Chap. 1.

[3]Cacciatore, M., Capitelli, M., DeBenedictis, S., Dilonardo, M., and Gorse, C., "Vibrational Kinetics, Dissociation and Ionization of Diatomic Molecules Under Nonequilibrium Conditions," *Nonequilibrium Vibrational Kinetics*, Springer–Verlag, Berlin, 1986, pp. 5–46, Chap. 2.

[4]Park, C., *Nonequilibrium Hypersonic Aerodynamics*, Wiley, New York, 1990, Chap. 3.

[5]Rapp, D., and Kassal, T., "The Theory of Vibrational Energy Transfer Between Simple Molecules in Nonreactive Collisions," *Chemical Reviews*, Vol. 69, No. 1, 1969, pp. 61–102.

[6]Nikitin, E. E., and Osipov, A. I., "Vibrational Relaxation in Gases," *Kinetics and Catalysis*, Vol. 4, VINITI, All-Union Inst. of Scientific and Technical Information, Moscow, 1977, Chap. 2.

[7]Secrest, D., "Vibrational Excitation I: The Quantal Treatment," *Atom-Molecule Collision Theory*, Plenum, New York, 1979, pp. 377–390, Chap. 11.

[8]Gentry, W. R., "Vibrational Excitation II: Classical and Semiclassical Methods," *Atom-Molecule Collision Theory*, Plenum, New York, 1979, pp. 391–412, Chap. 12.

[9]Billing, G. D., "Vibration-Vibration and Vibration-Translation Energy Transfer, Including Multiquantum Transitions in Atom-Diatom and Diatom-Diatom Collisions," *Nonequilibrium Vibrational Kinetics*, Springer–Verlag, Berlin, 1986, pp. 85–111, Chap. 4.

[10]Bogdanov, A. V., Dubrovskii, G. V., Gorbachev, V. E., and Strelchenya, V. M., "Theory of Vibrational and Rotational Excitation of Polyatomic Molecules," *Physics Reports*, Vol. 181, No. 3, 1989, pp. 121–206.

[11]Deleon, R., and Rich, J. W., "Vibrational Energy Exchange Rates in Carbon Monoxide," *Chemical Physics*, Vol. 107, No. 2, 1986, pp. 283–292.

[12]Yang, X., Kim, E. H., and Wodtke, A. M., "Vibrational Energy Transfer of Very Highly Vibrationally Excited NO," *Journal of Chemical Physics*, Vol. 96, No. 7, 1992, pp. 5111–5122.

[13]Price, J. M., Mack, J. A., Rogaski, C. A., and Wodtke, A. M., "Vibrational-State-Specific Self-Relaxation Rate Constant Measurements of Highly Excited $O_2(v = 19–28)$," *Chemical Physics*, Vol. 175, No. 1, 1993, pp. 83–98.

[14]Park, H., and Slanger, T. G., "$O_2(X, v = 8–22)$ 300 K Quenching Rate Coefficients for O_2 and N_2 and $O_2(X)$ Vibrational Distribution from 248 nm O_3 Photodissociation," *Journal of Chemical Physics*, Vol. 100, No. 1, 1994, pp. 287–300.

[15]Klatt, M., Smith, I. W. M., Tuckett, R. P., and Ward, G. N., "State-Specific Rate Constants for the Relaxation of $O_2(X^3\Sigma_g^-)$ from Vibrational Levels $v = 8$ to 11 by Collisions with NO_2 and O_2," *Chemical Physics Letters*, Vol. 224, Nos. 3, 4, 1994, pp. 253–257.

[16]Secrest, D., and Johnson, B. R., "Exact Quantum Mechanical Calculations of a Collinear Collision of a Particle with a Harmonic Oscillator," *Journal of Chemical Physics*, Vol. 45, No. 12, 1966, pp. 4556–4570.

[17]Chapuisat, X., Bergeron, G., and Launay, J.-M., "A Quantum-Mechanical Collinear Model Study of the Collision N_2O_2," *Chemical Physics*, Vol. 20, No. 2, 1977, pp. 285–298.

[18]Chapuisat, X., and Bergeron, G., "Anharmonicity Effects in the Collinear Collision of Two Diatomic Molecules," *Chemical Physics*, Vol. 36, No. 3, 1979, pp. 397–405.

[19]Billing, G. D., and Fisher, E. R., "VV and VT Rate Coefficients in H_2 by a Quantum-Classical Model," *Chemical Physics*, Vol. 18, Nos. 1, 2, 1976, pp. 225–232.

[20]Billing, G. D., and Fisher, E. R., "VV and VT Rate Coefficients in N2 by a Quantum-Classical Model," *Chemical Physics*, Vol. 43, No. 3, 1979, pp. 395–401.

[21]Billing, G. D., and Kolesnick, R. E., "Vibrational Relaxation of Oxygen. State to State Rate Constants," *Chemical Physics Letters*, Vol. 200, No. 4, 1992, pp. 382–386.

[22]Billing, G. D., "VV and VT Rates in N_2O_2 Collisions," *Chemical Physics*, Vol. 179, No. 3, 1994, pp. 463–467.

[23]Billing, G. D., "Vibrational/Vibrational Energy Transfer in CO Colliding with $^{14}N_2$, $^{14}N^{15}N$, and $^{15}N_2$," *Chemical Physics*, Vol. 50, No. 2, 1980, pp. 165–173.

[24]Cacciatore, M., and Billing, G. D., "Semiclassical Calculations of VV and VT Rate Coefficients in CO," *Chemical Physics*, Vol. 58, No. 3, 1981, pp. 395–407.

[25]Herzfeld, K. F., and Litovitz, T. A., *Absorption and Dispersion of Ultrasonic Waves*, Academic, New York, 1959, Chap. 3.

[26]Rapp, D., and Sharp, T. E., "Vibrational Energy Transfer in Molecular Collisions Involving Large Transition Probabilities," *Journal of Chemical Physics*, Vol. 38, No. 11, 1963, pp. 2641–2648.

[27]Rapp, D., and Englander-Golden, P., "Resonant and Near-Resonant Vibrational-Vibrational Energy Transfer Between Molecules in Collisions," *Journal of Chemical Physics*, Vol. 40, No. 2, 1964, pp. 573–575.

[28]Rapp, D., and Englander-Golden, P., "Erratum: Resonant and Near-Resonant Vibrational-Vibrational Energy Transfer Between Molecules in Collisions," *Journal of Chemical Physics*, Vol. 40, No. 10, 1964, pp. 3120–3121.

[29]Rapp, D., "Interchange of Vibrational Energy Between Molecules in Collisions," *Journal of Chemical Physics*, Vol. 43, No. 1, 1965, pp. 316, 317.

[30]Sharma, R. D., and Brau, C. A., "Energy Transfer in Near-Resonant Molecular Collisions due to Long-Range Forces with Application to Transfer of Vibrational Energy from ν_3 Mode of CO_2 to N_2," *Journal of Chemical Physics*, Vol. 50, No. 2, 1969, pp. 924–930.

[31]Kerner, E. H., "Note of the Forced and Damped Oscillations in Quantum Mechanics," *Canadian Journal of Physics*, Vol. 36, No. 3, 1958, pp. 371–377.

[32]Treanor, C. E., "Vibrational Energy Transfer in High Energy Collisions," *Journal of Chemical Physics*, Vol. 43, No. 2, 1965, pp. 532–538.

[33]Zelechow, A., Rapp, D., and Sharp, T. E., "Vibrational-Vibrational-Translational Energy Transfer Between Two Diatomic Molecules," *Journal of Chemical Physics*, Vol. 49, No. 1, 1968, pp. 286–299.

[34]Cottrell, T. L., and Ream, N., "Transition Probability in Molecular Encounters Part I. The Evaluation of Perturbation Integrals," *Transactions of the Faraday Society*, Vol. 51, No. 1, 1955, pp. 159–171.

[35]Heidrich, F. B., Wilson, K. R., and Rapp, D., "Collinear Collisions of an Atom and Harmonic Oscillator," *Journal of Chemical Physics*, Vol. 54, No. 9, 1971, pp. 3885–3897.

[36]McKenzie, R. L., "Vibration-Translation Energy Transfer in Anharmonic Diatomic Molecules," *Journal of Chemical Physics*, Vol. 63, No. 4, 1975, pp. 1655–1662.

[37]Gentry, W. R., and Giese, C. F., "Quantum Vibrational Transition Probabilities from Real Classical Trajectories: Collinear Atom-Diatom Collisions," *Journal of Chemical Physics*, Vol. 63, No. 7, 1975, pp. 3144–3155.

[38]Skodje, R. T., Gentry, W. R., and Giese, C. F., "Quantum Vibrational Transition Probabilities from Real Classical Trajectories: Symmetric Diatom-Diatom Collisions," *Journal of Chemical Physics*, Vol. 66, No. 1, 1977, pp. 160–168.

[39]Skodje, R. T., Gentry, W. R., and Giese, C. F., "Quantum Vibrational Transition Probabilities from Real Classical Trajectories: Asymmetric Diatom-Diatom Collisions," *Chemical Physics*, Vol. 74, No. 3, 1983, pp. 347–364.

[40]Gradshtein, I. S., and Ryzhik, I. M., *Tables of Integrals*, Nauka, Moscow, 1971.

[41]Keck, J., and Carrier, G., "Diffusion Theory of Nonequilibrium Dissociation and Recombination," *Journal of Chemical Physics*, Vol. 43, No. 7, 1965, pp. 2284–2298.

[42]Poulsen, L. L., and Billing, G. D., "Calculation of Vibrational Deactivation of $HF(1 \leq n \leq 7)$ by DF(0) and of $DF(1 \leq n \leq 7)$ by HF(0)," *Chemical Physics*, Vol. 36, No. 2, 1979, pp. 271–281.

[43]Nikitin, E. E., *Theory of Elementary Atomic and Molecular Processes in Gases*, Clarendon, Oxford, England, UK, 1974, Chap. 3.

[44]Kelley, J. D., "Vibrational Energy Transfer Processes in Collision Between Diatomic Molecules," *Journal of Chemical Physics*, Vol. 56, No. 12, 1972, pp. 6108–6117.

[45]Riley, M. E., and Kupperman, A., "Vibrational Energy Transfer in Collisions Between Diatomic Molecules," *Chemical Physics Letters*, Vol. 1, No. 11, 1968, pp. 537, 538.

[46]Clarke, J. H., and Thiele, E., "The Collinear Collision of Two Diatomic Molecules. An Application of the Adiabatic Approximation and the T- and K-Matrix Methods," *Chemical Physics*, Vol. 4, No. 3, 1974, pp. 447–457.

[47]Gutschnik, V., McKoy, V., and Diestler, D., "Calculation of Transition Probabilities for Collinear Atom-Diatom and Diatom-Diatom Collisions with Lenard-Jones Interaction," *Journal of Chemical Physics*, Vol. 52, No. 9, 1970, pp. 4807–4817.

[48]Mies, F. H., "Effects of Anharmonicity on Vibrational Energy Transfer," *Journal of Chemical Physics*, Vol. 40, No. 2, 1964, pp. 523–531.

[49]Dmitrieva, I. K., Pogrebnya, S. K., and Porshnev, P. I., "V-T and V-V Rate Constants for Energy Transfer in Diatomics. An Accurate Analytical Approximation," *Chemical Physics*, Vol. 142, No. 1, 1990, pp. 25–33.

[50]Kuksenko, B. V., and Losev, S. A., "On the Theory of Vibrational Relaxation of Diatomic Molecules," *High Temperature*, Vol. 6, No. 5, 1968, pp. 794–799.

[51]Taylor, R. L., and Bitterman, S., "Survey of Vibrational Relaxation Data for Processes Important in the CO_2-N_2 Laser System," *Reviews of Modern Physics*, Vol. 41, No. 1, 1969, pp. 26–47.

[52]Adamovich, I. V., Macheret, S. O., Rich, J. W., and Treanor, C. E., "Vibrational Relaxation and Dissociation Behind Shock Waves Part 2: Master Equation Modeling," *AIAA Journal*, Vol. 33, No. 6, 1995, pp. 1070–1075.

[53]Treanor, C. E., Adamovich, I. V., Williams, M. J., and Rich, J. W., "Kinetics of Nitric Oxide Formation Behind Shock Waves," *Journal of Thermophysics and Heat Transfer*, Vol. 10, No. 2, 1996, pp. 193–199.